Plasma Chemistry and Plasma Processing (2021) 41:1517–1534
https://doi.org/10.1007/s11090-021-10196-1

ORIGINAL PAPER

Experimental Study on the Restrike Mode of a DC Arc Anode Attachment

Ke Shao[1,2] · Ya-Hao Hu[1,2] · Xian Meng[2] · He-Ji Huang[2] · Su-Rong Sun[1,3] · Hai-Xing Wang[1,3]

Received: 10 February 2021 / Accepted: 17 June 2021 / Published online: 28 June 2021

Abstract

The restrike mode is an important arc anode attachment mode under the cross flow in DC arc device, which often causes a large amplitude of arc voltage fluctuations and therefore has an important impact on the performance of arc thermal plasma device. A transferred arc device with planar anode parallel to gas flow direction is used to experimentally study the restrike mode characteristics under different operating conditions. It is found that for the case of a fixed gas flow, the arc restrike frequency increases while the amplitude of arc voltage jump decreases with the increase of arc current. For the case of a fixed arc current, both arc restrike frequency and amplitude of arc voltage jump increase with the increase of gas flow rates. Further analysis shows that the restrike process in one period can be divided into two phases. The first phase corresponds to the generation and development of upstream new arc roots and the disappearance of downstream old root, and its time scale is less than the order of 1 ms. The second phase corresponds to the newly formed, single arc root moving downstream under the combined action of gasdynamic drag force and Lorentz force until new arc root appears upstream. The time-resolved temperature field measurement based on the relative intensity of emission spectrum method shows that the temperature at the junction of the arc column and the anode arc root is relatively low, while it still able to maintain the current conduction, which indicates the significant deviation from thermodynamic equilibrium state.

Keywords Arc anode attachment · Restrike mode · Arc root

✉ Xian Meng
mengxian@imech.ac.cn

✉ Hai-Xing Wang
whx@buaa.edu.cn

[1] School of Astronautics, Beihang University, Beijing 100191, China

[2] Institute of Mechanics, Chinese Academy of Sciences, Beijing 100190, China

[3] Ningbo Institute of Technology, Beihang University, Ningbo 315800, China

Introduction

As a high-temperature heat source, the DC arc plasma devices have extensive applications in the fields of spraying, material synthesis and waste treatment. In the typical non-transferred arc plasma torch commonly used in industry, the rod-shaped cathode is arranged in parallel with the anode channel, which causes the gas flow direction to be perpendicular to the arc attached to the anode surface. The arc anode attachment is exposed to strong gasdynamic drag force exerted by the cold flow, thus presenting different arc attachment modes, such as the steady, takeover, and restrike mode [1–6]. Different arc anode attachment modes are closely related to the torch operating voltage, especially the restrike attachment mode. The corresponding large magnitude of arc voltage fluctuation directly affects the power output, arc and jet characteristics, which has a great influence on the performance of the torch. Therefore, the study on the restrike mode of arc anode attachment has been received extensive and continuous attention by the thermal plasma community [7–16].

The emergence of the restrike mode of arc in cross flow is mainly caused by the competition between a pulling down drag force exerted by the cold flow in the boundary layer and the Lorentz force due the self-magnetic field induced by the curvature of the current flow [1, 17]. When the flow rate of cold gas is greater than a certain critical value, the arc root is pushed downstream under the combined action of gasdynamic drag force and Lorentz force, accompanying with the increase of arc length and the arc voltage. If the arc voltage reaches a certain value, the breakdown phenomenon at a certain upstream position occurs again, the arc is attached to the upstream again. And then the arc length is shortened, and the arc voltage drops. Arc anode attachment position, *i.e*., arc anode root, moves back and forth along the anode surface leading to the familiar sawtooth-like waveform of arc voltage. Duan et al. [18] developed a method of observing and estimating the thickness of the cold boundary layer and the attachment position of the arc root at the end of the non-transferred torch using a high-speed camera. They found that a thicker cold boundary layer tends to cause arc restrike mode, while a thinner cold boundary layer tends to maintain a steady state arc attachment mode. However, in this kind of non-transferred plasma torch, the movement and dynamic behavior of the arc anode attachment cannot be directly observed. Yang and Heberlein [19, 20] developed a wall-stabilized transferred arc device, so they can directly observe the arc anode attachment behavior under the action of lateral gas flows. In their study, they focus on the transition from a steady mode to a takeover mode and finally to a restrike mode. It was found that electron overheating instability plays an important role during the transition, and it is driving mechanism for the transition of anode attachment in arcs without cross flow [12, 21, 22]. It should be noted that in their experimental device [19, 20], the direction of the anode plate is perpendicular to the cathode, causing the direction of the cathode jet to be perpendicular to the anode. This electrode arrangement is different from the commonly used non-transferred arc torch. The most similar electrode arrangement to a non-transferred arc torch is that the anode is parallel to the cathode axis and gas flow direction. Previous experiments in [1, 17] have adopted this arrangement, but their researches focus on the influence of different attachment modes on anode heat transfer.

For arcs in cross flow, the arc is actually composed of cathode jets and anode jets connected to each other. Under the gasdynamic drag force of the cold air flow in the boundary layer, the anode arc column bends and the arc root moves downstream. The mutual evolution of the cathode and anode arc columns determines the overall characteristics of the arc. For the establishment of the arc root position prediction model and further analysis, it

is important to obtain information about the upstream position of the arc restrike, the arc root movement range and the relationship with the arc voltage [23]. Previous experiments and theoretical analysis have demonstrated the close relationship between the thickness of the boundary layer and the restrike process [24–27]. It is necessary to further investigate the effects of arc current and gas flow on restrike characteristics such as arc root movement range and frequency. Since the arc restrike process occurs in the order of several milliseconds, it is also very important to further distinguish the generation, development of new arc root and disappearance of old arc root in a shorter time scale for the development of physical models that consider thermodynamic and chemical non-equilibrium processes.

Based on the above discussion, the main purpose of this study is to study the arc restrike characteristics in the cross flow. The specific device with a rod-shaped cathode and an anode flat plate parallel to the axis of cathode can be used to directly observe the dynamic behavior of the arc under the action of cold flow, which is similar to the device used in Refs. [1, 17]. This electrode arrangement can make the arc-gas-electrode interaction basically consistent with that inside the non-transferred plasma torch and it would help to improve the understanding of the restrike process in the non-transferred plasma torch.

Experimental Setup

The general layout of the transferred arc device used in this study is shown schematically in Fig. 1. The experimental chamber with a diameter of 600 mm and a height of 550 mm is used to maintain one atmospheric pressure with argon atmosphere as the arc working gas. The electrode arrangement of the transferred arc device is shown on the right side of Fig. 1. This transferred arc device includes a thorium tungsten cathode with diameter of 5 mm, and a 60-degree cone angle at the tip, a copper anode which is parallel to the cathode axis, the distance of the anode and the cathode axis is 7 mm. The cathode and anode are separately water-cooled by a water-cooling system. The working gas is supplied through the channel between the cathode and the alumina ceramic cover, and the flow rate can be controllably adjusted from 5 to 30 slm (standard liter per minute). The power supply adopts an IGBT inverter DC constant current power supply, and the current adjustment range is 40–160 A.

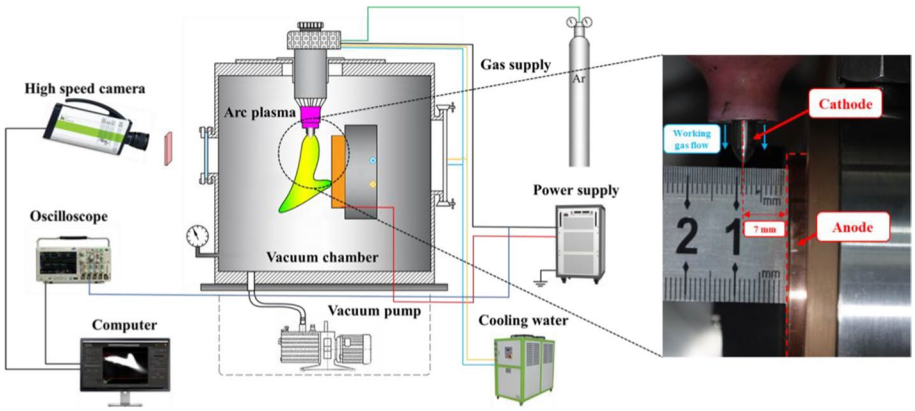

Fig. 1 Schematic diagram of transferred arc device and electrode configuration

In order to better observe the arc dynamic behavior under the action of the cold argon flow, a monochromatic high-speed camera, an i-SPEED 513, with a frame rate of 50,000 fps, a pixel resolution of 504 × 282, and an exposure time of 1 μs is used in this study. This frame rate is high enough to observe the rapid movement of arc root around the anode during the restrike process. A Nikon prime camera lens (adjustable aperture range is f1.4 ~ 16) is used together with a 64 × center density filter. The focal length is 50 mm and the distance between the lens and the anode plate is about 0.5 m.

The arc voltage for this device is obtained by measuring the voltages between the electrodes, using a voltage probe (Textronix TPP0500B) and a digital oscilloscope (Textronix MDO3034). During the experiment, the shooting of arc dynamic behavior and the measurement of arc voltage data were synchronized in order to analyze their relations.

The temperature evolution of the arc during restrike can provide more useful information and help us deepen our understanding of the physical processes involved in the arc root movement. In this study, an in situ measurement of the two-dimensional temperature field of arc plasma reported in [28–31] is adopted. This temperature field time-resolved measurement system consists of a special optical assembly, a high-speed camera and associated software. The main principle of this measurement method is based on the arc image processing technology and the relative intensity ratio of two specific spectral lines. By calibrating with the emission intensity measured by the spectrometer, we can convert the gray value recorded by the high-speed camera with different narrow band filters into the temperature distribution of the arc plasma.

Calibration is the basis for obtaining accurate and reasonable temperature measurement. In order to ensure the consistency of the measured and calibrated temperature fields, the measured intensity distribution of the arc emission during the restrike process should be used as the calibration object itself. However, since the restrike process evolves with time very quickly, it is very difficult to directly measure the distribution of the emission intensity of arc in the high-speed motion. Therefore, in this study, we use a stable free burning arc system as the emission spectrum temperature measurement calibration setup, as shown in Fig. 2. In order to ensure as much as possible the consistency of the emission intensity and distribution of a free burning plasma arc with those of the arc in restrike process in this study, we adopt the electrode structure, plasma forming gas and operating parameters such as the arc current and gas flow rate, are the same with those in measured restrike process.

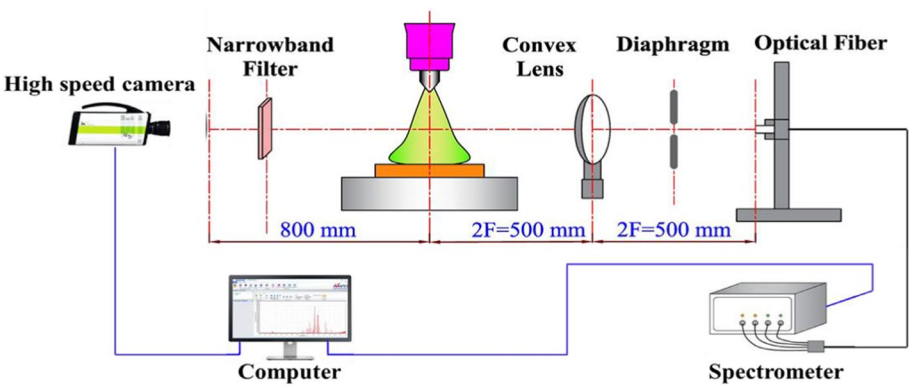

Fig. 2 Schematic of arc plasma optical emission spectrum diagnostics calibration setup

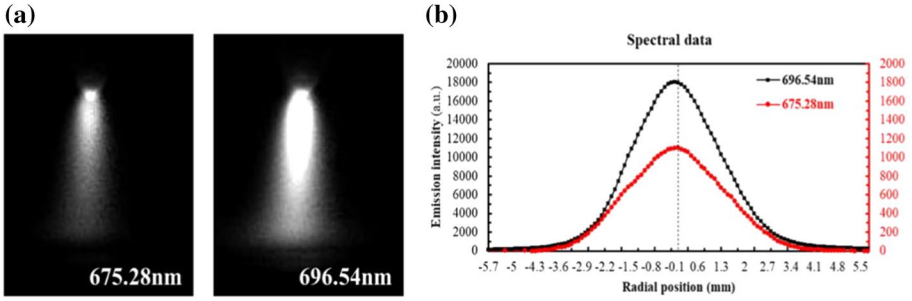

Fig. 3 **a** Two images of the free-burning argon arc recorded by high-speed camera with two narrow band filters at the wavelengths of 675.28 nm and 696.54 nm, **b** Emission intensity distribution of the free-burning argon arc synchronously recorded by spectrometer (arc current 100 A, electrode gap 10 mm, argon flow rate 10 slm)

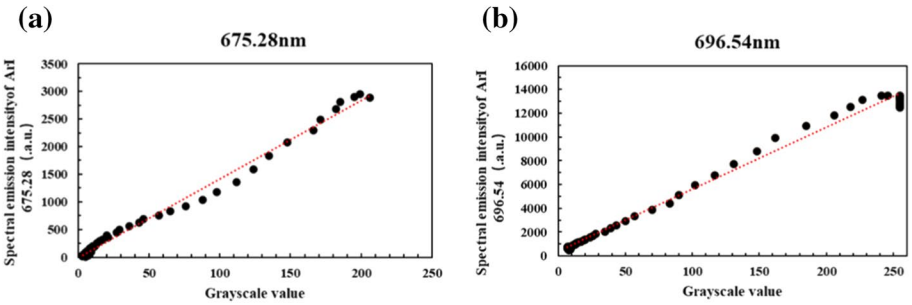

Fig. 4 Relationship between the spectral emission intensity and gray scale value at wavelengths of **a** 675.28 nm, **b** 696.54 nm (arc current 100 A, electrode gap 10 mm, argon flow rate 10 slm)

Figure 3a presents the images of the free-burning argon arc recorded by high-speed camera with two narrow band filters at the wavelengths of 675.28 nm and 696.54 nm with band width of 10 nm. At the same time, the emission intensity distributions at these two wavelengths of this free-burning argon arc are synchronously recorded by a four-channel spectrometer (AvaSpec-ULS4096CL) as shown in Fig. 3b. It is worth noting that in the Ref. [29], the two grayscale images corresponding to the two spectral lines were taken simultaneously by two CCD cameras through two narrowband filters. However, in our experiments, we found that the state of the free burning arc is very stable, that is, the temperature field does not change during the time we measured. So here, Fig. 3a is taken by using a fixed-position monochrome high-speed camera and changing two-wavelength narrow-band filters twice. The radial intensity distributions of the two specific emission spectrum lines are recorded at the axis 0.5 mm below the cathode. Find the gray value at the corresponding position of the gray image taken by a monochrome high-speed camera in the Fig. 3a, we can establish the corresponding relationship between emission intensity and gray value, as shown in Fig. 4.

The variations of emission intensity and the corresponding gray scale at the two wavelengths of a free-burning arc are shown in Fig. 4. With a further linear fitting, the following relation between the emission intensity and value of gray scale can be obtained

$$I_1 = 14.22G_1 - 4.78 \tag{1}$$

$$I_2 = 49.61G_2 + 453.71 \tag{2}$$

Here, the I is emission intensity, and G represents the value of gray scale. Based on the assumption of thermodynamic equilibrium, using the relative intensity method, the temperature of the arc plasma can be determined according to the following formula

$$T_g = \frac{E_1 - E_2}{k_B\left(\ln\frac{g_1A_1\lambda_2}{g_2A_2\lambda_1} - \ln\frac{I_1}{I_2}\right)} \tag{3}$$

As mentioned above, the two selected wavelengths are respectively $\lambda_1 = 675.28$ nm and $\lambda_2 = 696.54$ nm. In Eq. (3), the E_1 and E_2 respectively represent the upper energy level, which are taken as 14.74 eV and 13.33 eV. g_i and A_i are statistical weight and Einstein transition probability for the transition wavelength. The g_1A_1 and g_2A_2 are respectively taken as 9.65×10^6 and 1.92×10^7 s^{-1} [32]. Since we have established the relationship between gray value and light intensity as in formulas (1) and (2), we can take the gray value of each pixel of two wavelength in the arc restrike process taken by a monochrome high-speed camera and respectively match them to the intensity values of two spectral lines. And then, substituting the emission intensity value into Eq. (3), we can get the temperature value of each point in the two-dimensional temperature field. More detailed information about the matching methods between the grayscale and emission intensity can be found in the Ref. [29].

Experimental Results and Discussion

Effects of Arc Current on the Restrike Process

Figure 5 shows the movement of the arc root along the anode when the argon flow rate keeps to be 10 slm while the arc currents are set to be 50, 100, and 150 A respectively. In order to facilitate analysis and comparison, the arc images in Fig. 5 are collected using the same shooting conditions. From the high-speed photographs taken in the experiment, it is found that under such electrode arrangement and operating conditions, the arc moves periodically along the anode surface. As shown in the Fig. 5, when the original arc root, with the label of R1, moves downstream, the arc voltage increases as the arc length increases. When the R1 moves to a certain position downstream, at a certain upstream position, the electric field strength also increases to a critical value, causing the arc to break-down again, thereby forming a new arc root, with the label of R2. The whole process is repeated continuously to form a restrike mode of the arc anode attachment.

It is also seen from Fig. 5 that when the arc current is 50 A, the gasdynamic drag force of the cold flow has a greater impact on the attachment position of the arc anode and the range of motion of the arc root. Because the current is relatively small, both the arc columns of cathode and anode are very thin, and the connection between the cathode arc column and the anode arc column is obviously bent downstream under the combined action of gasdynamic drag and Lorentz force. When the arc current increases to 100 A and 150 A, the diameters of the anode and cathode arc columns also increase and the arc root movement range between upstream and downstream decreases during periodic

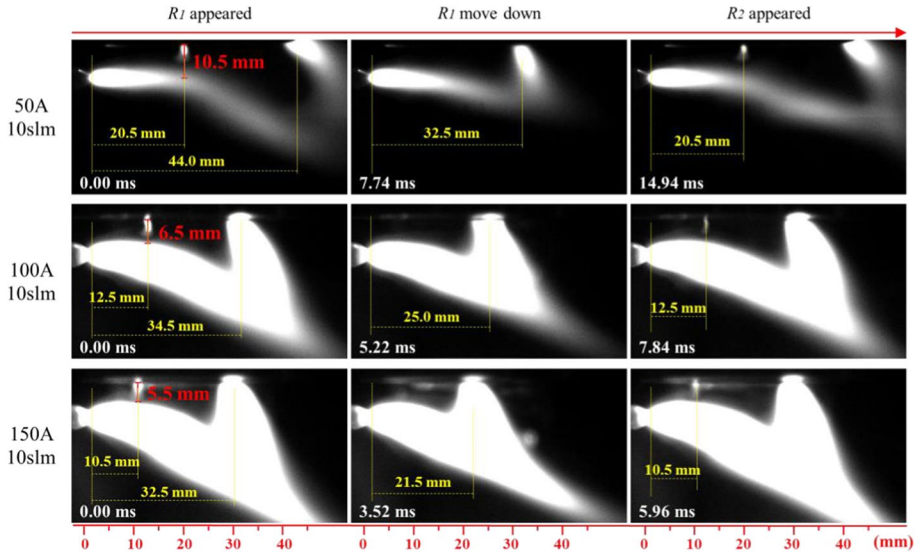

Fig. 5 Frames from high-speed movie of argon in restrike mode within one period, arc currents of 50, 100, and 150 A, argon flow rate of 10 slm

restrike processes. It should be also noted that as the current increases, the arc restrike position, where the new arc root appears, also moves upstream. Changes in upstream arc restrike position can be correlated with changes in thickness of cold boundary layer.

The evolution of the cold boundary layer thickness with current can also be seen in the first column of the Fig. 5. Taking the position of the upstream arc attachment point during the restrike process as an example, the edge cold boundary layer is defined as the location with 65% of the maximum emission intensity (65% of the maximum gray value 255 i.e. 166 for all the cases with different operating conditions) on the local section. The similar method is also used to estimate the thickness of cold boundary layer of the arc inside the nozzle for non-transferred plasma torch [18]. It can be seen from Fig. 5 that as the arc current increases from 50 to 150 A, the thickness of the cold boundary layer decreases from 10.5 to 5.5 mm. The change in thickness of the cold boundary layer mainly is connected with the degree of thermodynamic non-equilibrium inside it, the electron number density, and electron energy. For a thicker cold boundary layer, a higher electric potential drop i.e. longer distance between cathode and anode attachment position is required to reach the critical electric field strength and induce the gas breakdown. For a thinner boundary layer, the same potential difference between arc and anode position would cause a higher field making a breakdown more probable, the arc restrike position moves upward.

The typical sawtooth voltage fluctuation corresponding to the restrike mode of arc anode attachment for different arc currents can be seen in Fig. 6. The peak value of the voltage corresponds to the situation that the arc root moves to the critical position downstream of the anode, before the moment that arc root restrikes at the upstream position. The lowest value of voltage corresponds to the situation that the old arc root disappears, and the new arc root becomes the main body of the current channel. It can be clearly seen from the Fig. 6 that as the current increases, the frequency of arc restrike process increases, while the amplitude of voltage fluctuations decreases. The decrease

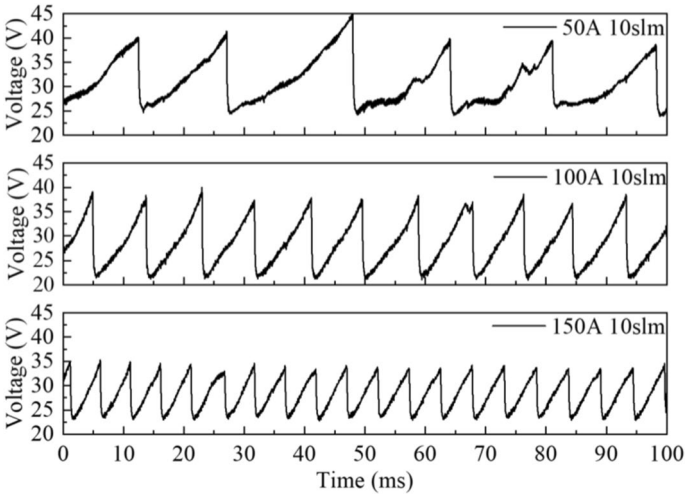

Fig. 6 Arc voltage waveforms of restrike processes corresponding to arc currents of 50, 100, and 150 A, gas flow rate of 10 slm

of the arc voltage fluctuations amplitude in the large current situation can be related to the decrease of the arc root's movement range between upstream and downstream, as shown in Fig. 5.

Variations of restrike frequency and amplitude of arc voltage jump with arc current are presented in Fig. 7. As mentioned above, with the increase of arc current, the restrike frequency increases while the amplitude of arc voltage jump during the restrike process decreases. This phenomenon has also been observed experimentally in the previous study [18, 23, 33–35]. Combined with Fig. 6 and Fig. 7, it can be estimated that the amplitude of the arc voltage jump is almost 20 ~ 40% of the total voltage.

Fig. 7 Variations of restrike frequency and amplitude of arc voltage jump with arc current, gas flow rate of 10 slm

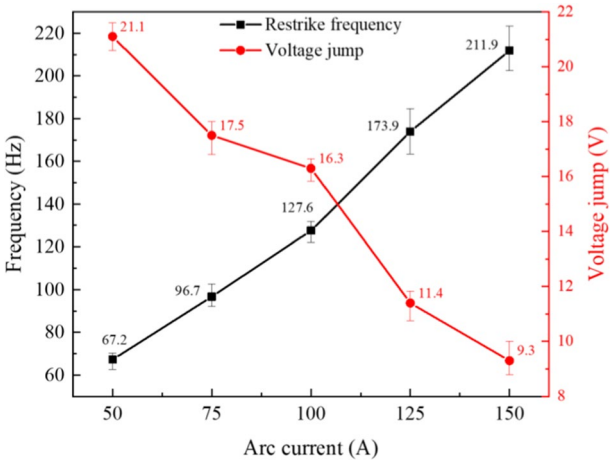

Effects of Gas Flow Rate on the Arc Restrike Process

Figure 8 presents the dynamic behavior of the arc during restrike process for the cases with the fixed arc current of 100 A while different gas flow conditions. It can be seen from the Fig. 8 that the gas flow has three effects on the dynamic behavior of the arc. Firstly, as the gas flow rate increases, the gasdynamic drag force increases, which leads to an increase of the distance from the upstream arc restrike position to the farthest arc root position downstream. Secondly, the arc restrike period decreases with the increase of gas flow rates. As the gas flow rate increases from 5 to 15 slm, the restrike period is shortened from 15.6 to 7.02 ms. Thirdly, the restrike position upstream of the arc moves downward as the gas flow increases. At the same time, as shown in the left column of Fig. 8, it is noted that under the condition with the fixed arc current, the radial size of the cathode arc column is basically unchanged, so the thickness of the cold boundary layer changes little.

The voltage fluctuation of arc anode attachment for restrike processes corresponding to different gas flow rates can be seen in Fig. 9. It can be seen from the Fig. 9 that in the case of small gas flow rate, the gasdynamic drag force in the cold boundary layer is relatively weak, and it takes a long time to push the arc root downstream, so it takes a long time to complete a restrike process. In the case of high gas flow, the gasdynamic force in the cold boundary layer is stronger, and a restrike process can be completed in a short time, so the restrike frequency increases.

Figure 10 presents the variations of restrike frequency and amplitude of arc voltage jump with the gas flow rates. Combined with the previous analysis, under the same arc current situation, the thickness of the cold boundary layer changes little with the gas flow rates as shown in Fig. 8. At this situation, the restrike frequency and the arc voltage jump amplitude are mainly affected by the changes in the gasdynamic drag force. Both restrike frequency and arc voltage jump amplitude increase with the increase of

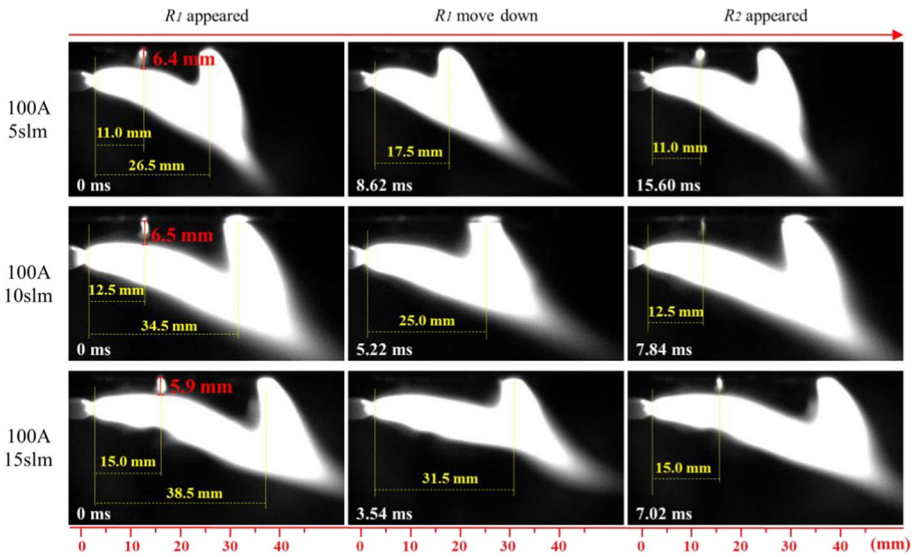

Fig. 8 Frames from high-speed movie of argon in restrike mode of operation within one period, arc current of 100 A, gas flow rates of 5, 10, 15 slm

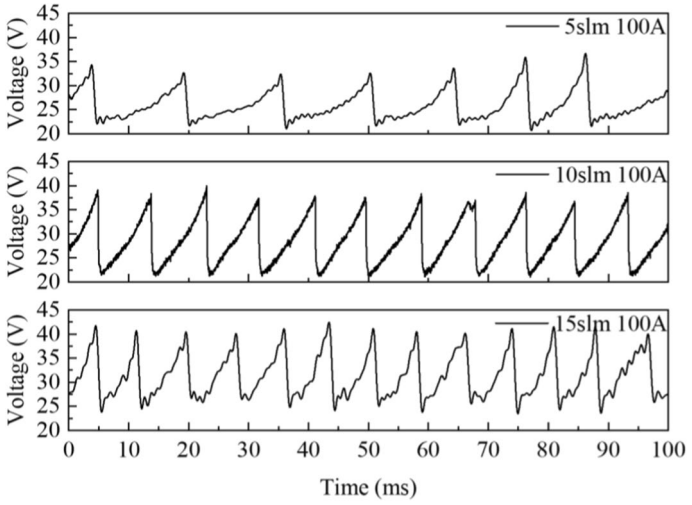

Fig. 9 Arc voltage waveforms of restrike processes under different gas flow rate (5 slm/10 slm/15 slm of argon) while the arc current fixed to be 100 A

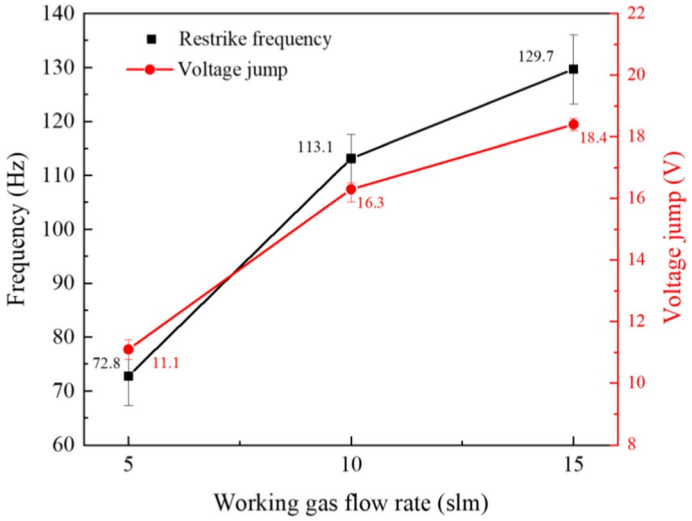

Fig. 10 Variations of restrike frequency and amplitude of arc voltage jump with gas flow rate, the arc current fixed to be 100 A

gas flow. Combined with Figs. 9, 10, it can be estimated that the amplitude of the arc voltage jump is almost 25 ~ 45% of the total voltage for different gas flow rates.

Analysis on the Dynamic Behavior of Anode Arc Root During Restrike Process

As mentioned above, the arc restrike process cycle is on the order of milliseconds, and a frame rate of 50,000 fps of high-speed camera is used in this experiment, indicating that

we can further observe the dynamic evolution of the arc on the time scale of 20 microsecond. Figure 11 shows the time evolution of arc restrike process in one period with the current of 100 A and the gas flow rate of 10 slm.

It can be seen from the Fig. 11 that after the upstream arc root appears, it takes 0.4 ms for the new arc root growing up. In the next 0.6 ms, the old arc root downstream gradually disappears, which means that the time scale of the current commutation between the new and old arc roots is smaller than 1 ms. In the following 6 ms of this period, the newly formed, single arc root gradually moves downstream under the combined action of gas-dynamic drag and Lorentz force. From the time evolution of the arc voltage in one period given in Fig. 12, the initial moment corresponds to the arc root movement to the downstream critical position, that is, the peak value of the arc voltage. By about 1.0 ms, the arc voltage has dropped to the lowest value. As can be seen from the corresponding Fig. 11,

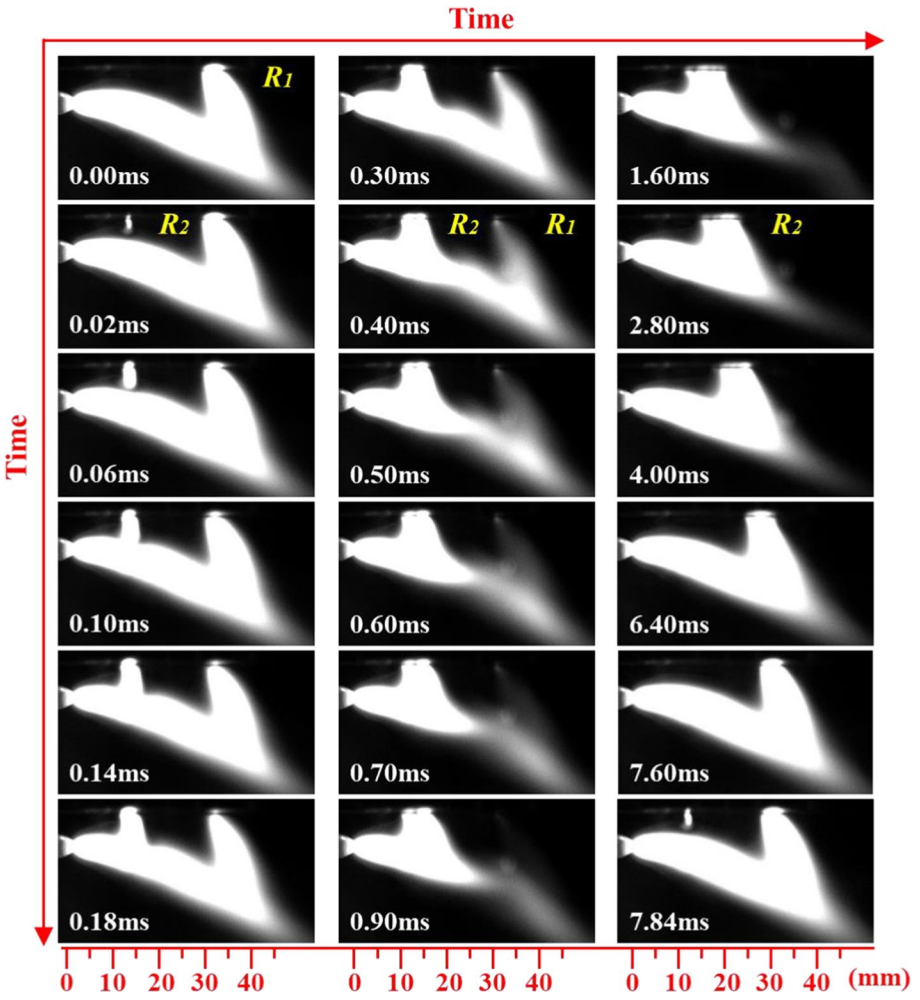

Fig. 11 Successive CCD images of arc movement for the case with arc current of 100 A, gas flow rate of 10 slm. R1, R2 denote anode attachment position

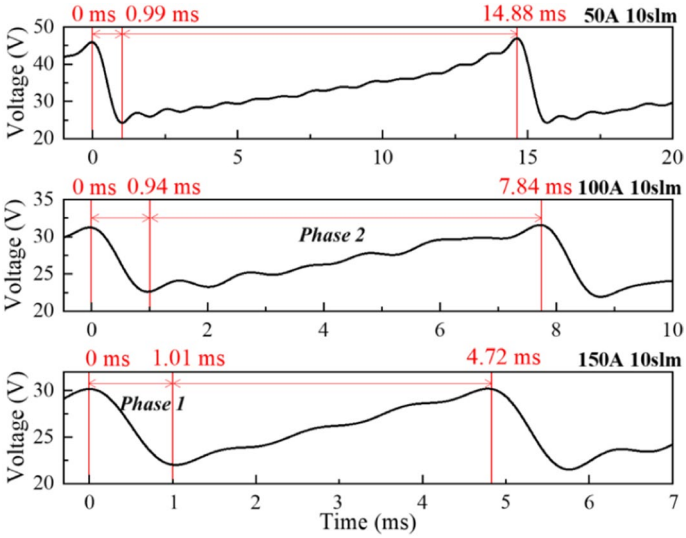

Fig. 12 Time evolution of the arc voltage during one period of restrike process, for the case with arc current of 50, 100, 150 A, argon flow rate of 10 slm

this corresponds to the moment when the old arc root disappears and formation of a new single arc root. This process can be named as the formation of new root, Phase 1 with time scale of 1 ms. In the following time of this period, the newly formed, single arc root moves downstream under the combined action of gasdynamic drag and Lorentz force, and arc voltage increase linearly with the increase of arc length. Therefore, this process can be named as the gas-dynamic drag force action Phase 2.

Note that in the Phase 1, in the process of the generation and development of the new upstream arc root, the gasdynamic drag force is not enough to push the arc root movement, so the position of the new arc root remains basically unchanged during this phase. The main physical process that occurs in Phase 1 is that the current is redistributed between the two arc roots under the driving of an electric field. In the Phase 2, the dominated process is that the newly formed arc root moves downstream under the combined action of gasdynamic drag and Lorentz force. According to the range and time of the arc root motion, it can be inferred that the arc root motion speed is around 1 ~ 4 m/s.

Figure 13 shows the evolution of arc roots during restrike processes within 1 ms under different operating currents. It can be seen from the Fig. 13 that although the formation time of new arc roots is slightly different, all of them can be finished within 1 ms. We have also checked the time required for the formation of new arc roots under different gas flow rates, and a similar time scale is found. It infers that the time required for Phase 1 is basically within 1 ms.

Preliminary Results of Time-resolved Measurement of Temperature Field During Restrike Processes

Due to the short time scale of the arc restrike process, time-resolved temperature measurement is quite difficult. Therefore, most of the experimental observations of the arc

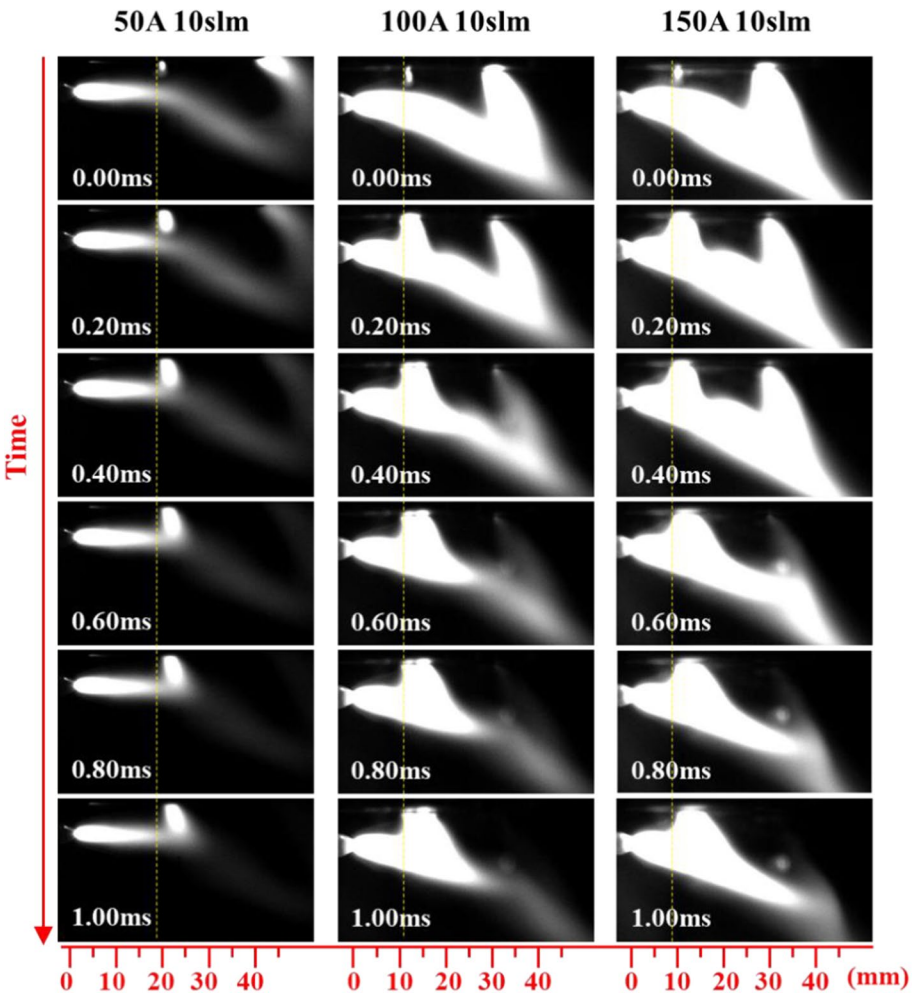

Fig. 13 Successive CCD images of arc movement within 1 ms, for the case with arc current of 50, 100, 150 A, gas flow rate of 10 slm

dynamic behavior reported in the literatures [2, 18] are based on grayscale pictures taken by a monochrome high-speed camera, and cannot provide information about the temperature distribution during the arc dynamic evolution. The temperature distribution during the dynamic evolution of the arc during the restrike process is helpful to understand the physical processes involved, and it also provides reference and verification for the corresponding theoretical analysis and numerical simulation. In this study, the temperature distribution of arc during the restrike processes is measured by the emission spectrum relative intensity measurement system described above. A typical temperature distribution at each moment with one period of the restrike process is shown in Fig. 14.

As mentioned above, using relative intensity method to measure temperature requires synchronously acquisition distribution information of two spectral lines, namely 675.28 nm and 696.54 nm. In order to ensure synchronization in the shooting process, it is reasonable to have two high-speed cameras with narrow band filters of 675.28 nm and 696.54 nm,

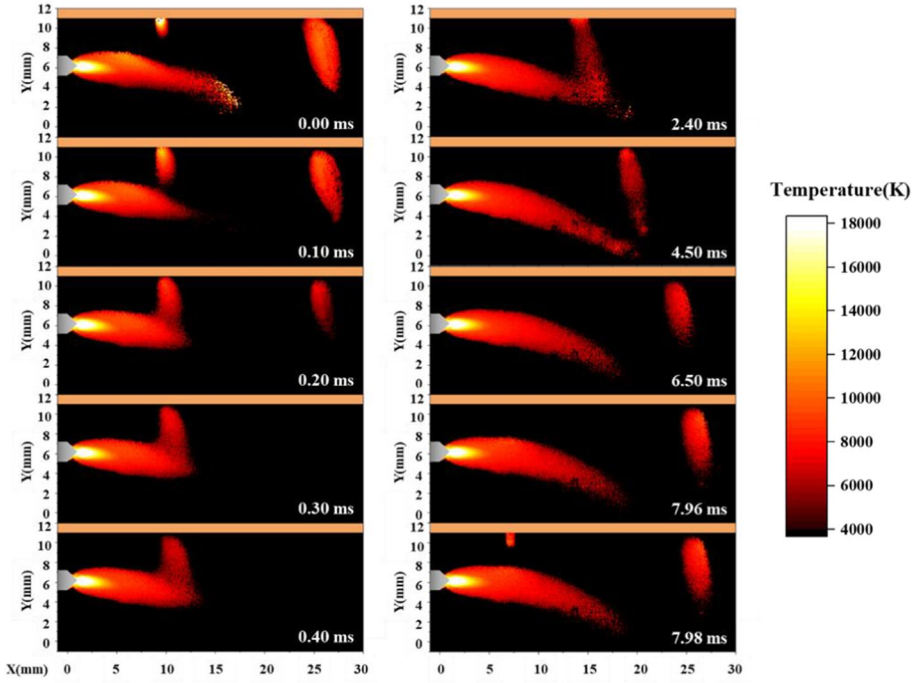

Fig. 14 The temperature distribution of the arc during a restrike period, for the case with arc current of 100 A, gas flow rate of 10 slm

respectively, to take photos at the same moment. However, in this experiment, by comparing the time–space distribution of arc and voltage waveform at the corresponding time in different periods taken by the high-speed camera, it was found that within the range of the operating parameters we measured, the space–time evolution distribution of the arc restrike process repeats very well in multiple periods. Therefore, in our experiment, a fixed-position monochrome high-speed camera is used. First, a 675.28 nm narrow-band filter is used to take photos of multiple cycles of arc restrike processes, and then replace it with a 696.54 nm narrow-band filter to take photos. After the photos are taken, we compare and select the best repeatability result of arc spatiotemporal evolution in one period from the pictures taken with two narrow band filters. Then on this basis, based on formulas (1)–(3), the temperature distribution of arc during restrike process can be calculated.

Comparing the gray-scale image information presented above and the temperature distribution of the arc dynamic evolution, it can be found that the connecting part of the cathode and downstream anode arc roots can be clearly observed in gray-scale photos in Figs. 5 and 8, while the cathode arc column and the downstream anode arc root seem to be separated in Fig. 14. The main reason is that the temperature distribution presented in Fig. 14 is obtained based on the thermodynamic equilibrium assumption. The emission intensity of the 675.28 nm and 696.54 nm lines at the junction of the cathode and anode arc columns is very weak. Although the temperature at the junction between the cathode and anode arc column is lower, the current can still be conducted, indicating that the downstream region of the arc is in a state that deviates significantly from the thermodynamic equilibrium.

It can also be observed from the Fig. 14 that when the arc restrikes upstream of the anode, although the size of the arc root is small, its temperature is very high and even equivalent to the temperature of the cathode arc column area, indicating that even at the initial moment of restrike, the current density of anode arc root is also very high. As the diameter of the anode arc column increases, the temperature of the anode arc column gradually decreases and keeps on the order of 8000 ~ 10000 K.

Figure 15 presents a comparison of the arc temperature distribution during the restrike process for different arc currents. In order to facilitate the comparison, the arc temperature color scale is uniformly set to 4000–18000 K for the three arc current conditions. It can be seen from the figure that the maximum temperature of the arc increases with the increase of the arc current, while the range of the high temperature region of the cathode jet becomes wider. It can also be seen from the figure that as the arc current increases, both the upstream restrike arc root position and the downstream arc root position gradually move upstream. It is also noted that for the cases of arc currents of 50 A and 100 A, the temperature and brightness at the connection of the cathode jet and the anode jet are very low, and it is difficult to obtain a reasonable temperature distribution in this region using this temperature measurement method.

It is worth noting that in the grayscale images given in Figs. 5, 8, and 11, based on the shooting conditions we used, the images in the high temperature area have been

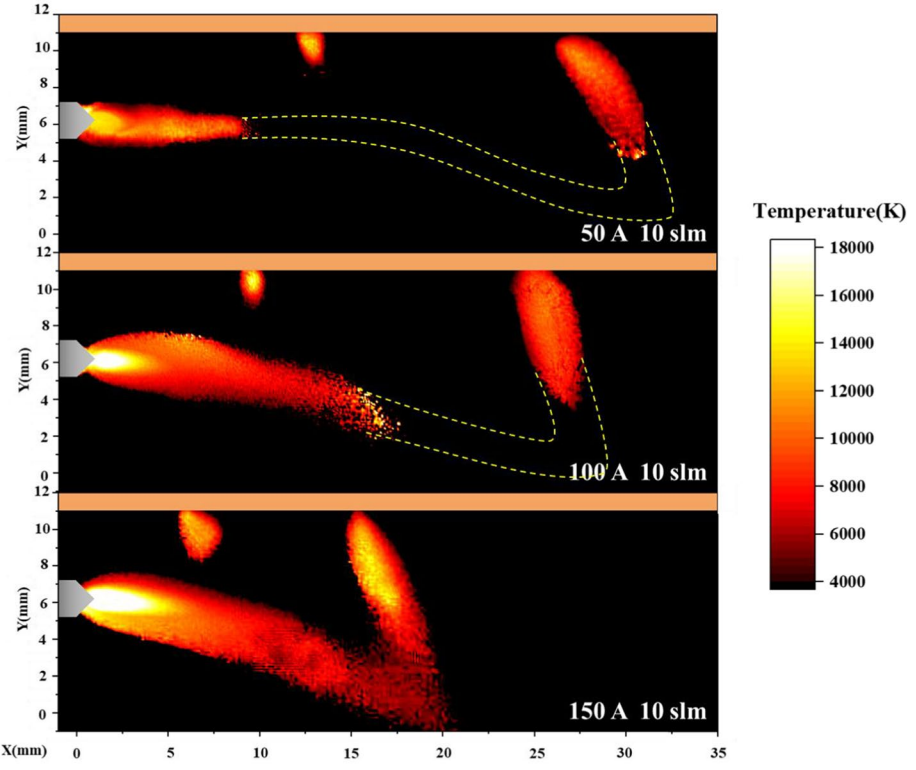

Fig. 15 The temperature distribution at the beginning of current commutation, for the case with arc current of 50 A, 100 A, 150 A, gas flow rate of 10 slm

overexposed. The result of the high temperature region (T > 15000 K) is actually obtained by linear extrapolation, which is one of the limitations of this method used in this study. Moreover, the temperature measurement is based on the relative intensity method and the image processing. The experimental errors could come from the calibration process and image matching process. In the calibration process, the emission superimposed along the line of sight is used to calculate the temperature rather than the real local emission after the spatial reconstruction by Abel-inversion since a large part of the arc region cannot be expected as rotaional symmetric in this experiment. The obtained temperature along the line of sight is between the maximum and the average temperature, which limits the accuracy of the measured arc temperature.

Although the accuracy of this time-resolved temperature measurement still has some extent of uncertainty, it still provides a reference for further theoretical analysis and numerical simulation. In the next step, the experimental measurement method can be improved by the beam splitting method, and it can be used to obtain the arc images under two different wavelength filters at the same time which is helpful to increase the accuracy of the experimental results. In this study, we use a transferred arc device to simulate the electrode configuration of a non-transferred arc, and the current parameters used are somewhat different from those of the actual non-transfer plasma torch, so the parameters such as the arc restrike frequency are also different. In this experiment, for arc currents of 50,100, 150 A, argon used as working gas, the measured arc restrike frequencies are 67, 127, and 212 Hz, respectively. It is noted that the experimental results for argon-helium non-transferred plasma torch [18], the measured restrike frequency is about 5 kHz for a current of 200 A, and the thickness of the boundary layer is about 1.2 mm. For argon–hydrogen non-transferred plasma torch [36], the measured restrike frequency is about 3.8 kHz for a current of 300 A. For the case with current of 500 A, the arc restrike frequency varies between 5 and 12 kHz as the gas flow rate increases [37]. Although these values of the restrike frequency and cold boundary layer thickness obtained from our experiments differ from the experimental measurements reported in the literature for non-transferred arc plasma torches, there is a great similarity in the physical process of arc restrike in both, which contributes to a better understanding of the restrike process of the arc anode attachment.

Conclusion

In this study, a transferred arc device with a plane anode parallel to the gas flow direction is used to study the restrike process and characteristics of DC arc anode attachment. High-speed photography is used to systematically observe the effects of gas flow and arc current on the characteristics of arc anode restrike. The relative intensity method of emission spectra is used to obtain the temperature distribution during the arc dynamic evolution in a period.

The experimental results show that when the current is small, the gasdynamic drag force has a greater influence on the arc shape, and the junction of the cathode and anode arc columns is obviously bent downstream. With the increase of arc current, the thickness of the anode cold boundary layer decreases, the position of arc restrike moves upstream, the frequency of arc restrike increases, and the amplitude of arc voltage jump decreases. Both restrike frequency and arc voltage jump amplitude increase with the increase of gas flow. It is found that the amplitude of the arc voltage jump is almost 25 ~ 45% of the total voltage for different gas flow rates.

Further analysis of the arc dynamic behavior in one restrike period shows that the dynamic evolution of the arc can be divided into two phases. The Phase 1 corresponds the generation and development of a new upstream arc root and disappearance of the old arc roots. In this phase, the size of new arc root upstream is small and the gas-dynamic drag force is not enough to push the arc root downstream, so the position of the upstream arc root remains basically unchanged. In the Phase 2, the newly formed single arc root gradually moves downstream under the combined action of gasdynamic drag force and Lorentz force. The time scale required in this Phase is on the order of several milliseconds.

Based on the relative intensity method of emission spectroscopy, a high-speed camera is used to obtain the temperature distribution during the dynamic evolution of the arc. The results show that the plasma significantly deviated from the thermodynamic equilibrium state at the junction between the cathode arc column and the downstream anode arc column. At the initial moment of the restrike process, the temperature of upstream arc root is as high as the temperature of cathode arc column region. With the development of the upstream anode arc root and the increase in size, the temperature of the arc anode attachment region gradually decreases to the order of 8000–10000 K.

Acknowledgements This work was supported by the National Natural Science Foundation of China (Grant Nos. 11735004, 12005010).

Data Availability The data that support the findings of this study are available from the corresponding author upon reasonable request.

References

1. Wutzke SA, Pfender E, Eckert ERG (2012) Study of electric arc behavior with superimposed flow. AIAA J 5(4):707–713
2. Heberlein JV, Mentel J, Pfender E (2010) The anode region of electric arcs: a survey. Journal of Physics D: Applied Physics 43(2):023001
3. Pan WX, Guo ZY, Meng X, Huang HJ, Wu CK (2009) Fluctuation characteristics of arc voltage and jet flow in a non-transferred DC plasma generated at reduced pressure. Plasma Sour Sci Technol 18(4):045032
4. Li HP, Heberlein JV, Pfender E (2005) Three-dimensional, nonequilibrium effects in a high-intensity blown arc. IEEE Trans Plasma Sci 33(2):402–403
5. Noguès E, Fauchais P, Vardelle M, Granger P (2007) Relation between the arc-root fluctuations, the cold boundary layer thickness and the particle thermal treatment. J Therm Spray Technol 16(5):919–926
6. Trelles JP, Heberlein JV, Pfender E (2007) Non-equilibrium modelling of arc plasma torches. J Phys D Appl Phys 40(19):5937–5952
7. Moreau E, Chazelas C, Mariaux G, Vardelle A (2006) Modeling the restrike mode operation of a DC plasma spray torch. J Therm Spray Technol 15(4):524–530
8. Shkol'Nik SM (2011) Anode phenomena in arc discharges: A review. Plasma Sour Sci Technol 20(1):013001
9. Chazelas C, Moreau E, Mariaux G, Vardelle A (2006) Numerical modeling of arc behavior in a DC plasma torch. High Temp Mater Processes (New York) 10(3):393–406
10. Huang HJ, Pan WX, Wu CK (2008) Arc root motion in an argon-hydrogen DC plasma torch. IEEE Trans Plasma Sci 36(4):1050–1051
11. Sun SR, Wang HX, Zhu T (2020) Numerical analysis of chemical reaction processes in different anode attachments of a high-intensity argon arc. Contrib Plasma Phys 60(3):1–11
12. Yang G, Heberlein JV (2007) Anode attachment modes and their formation in a high intensity argon arc. Plasma Sources Sci Technol 16(3):529–542
13. Pan WX, Li T, Meng X, Wu CK (2005) Arc root attachment on the anode surface of arc plasma torch observed with a novel method. Chin Phys Lett 022(011):2895–2898

14. Li HP, Pfender E, Chen X (2003) Application of Steenbeck's minimum principle for three-dimensional modelling of DC arc plasma torches. J Phys D Appl Phys 36(9):1084–1096
15. Sun SR, Kolev S, Wang HX, Bogaerts A (2017) Coupled gas flow-plasma model for a gliding arc: investigations of the back-breakdown phenomenon and its effect on the gliding arc characteristics. Plasma Sour Sci Technol 26(1):015003
16. Sun SR, Zhu T, Wang HX, Liu G, Murphy AB (2020) Three-dimensional chemical non-equilibrium simulation of an argon transferred arc with cross-flow. J Phys D: Appl Phys 53(30):305202
17. Eckert ERG, Pfender E, Wutzke SA (2012) Symptomatic behavior of an electric arc with a superimposed flow. AIAA J 6(8):1474–1482
18. Duan Z, Heberlein JV (2002) Arc instabilities in a plasma spray torch. J Therm Spray Technol 11(1):44–51
19. Yang G, Heberlein JV (2007) The anode region of high intensity arcs with cold cross flow. J Phys D Appl Phys 40(19):5649–5662
20. Yang G, Cronin P, Heberlein JV, Pfender E (2006) Experimental investigations of the anode boundary layer in high intensity arcs with cross flow. J Phys D Appl Phys 39(13):2764–2774
21. Yang G, Heberlein JV (2007) Instabilities in the anode region of atmospheric pressure arc plasmas. Plasma Sour Sci Technol 16(4):765–773
22. Huang HJ, Pan WX, Guo ZY, Wu CK (2010) Instabilities in a non-transferred direct current plasma torch operated at reduced pressure. J Phys D: Appl Phys 43(8):085202
23. Paik S, Huang PC, Heberlein JV, Pfender E (1993) Determination of the arc-root position in a DC plasma torch. Plasma Chem Plasma Process 13(3):379–397
24. Rat V, Mavier F, Coudert JF (2017) Electric arc fluctuations in DC plasma spray torch. Plasma Chem Plasma Process 37(3):549–580
25. Trelles JP, Pfender E, Heberlein JV (2006) Multiscale finite element modeling of arc dynamics in a DC plasma torch. Plasma Chem Plasma Process 26(6):557–575
26. Trelles JP, Pfender E, Heberlein JV (2007) Modelling of the arc reattachment process in plasma torches. J Phys D Appl Phys 40(18):5635–5648
27. Bhigamudre V, Trelles JP (2019) Characterization of the arc in crossflow using a two-temperature non-equilibrium plasma flow model. J Phys D: Appl Phys 52(1):015205
28. Ge N, Wu GQ, Li HP, Wang Z, Bao CY (2011) Evaluation of the two-dimensional temperature field and instability of a dual-jet DC arc plasma based on the image chain coding technique. IEEE Trans Plasma Sci 39(11):2884–2885
29. Guo H, Li P, Li HP, Ge N, Bao CY (2016) In situ measurement of the two-dimensional temperature field of a dual-jet direct-current arc plasma. Rev Scientific Instrum 87(3):053001
30. Wang Z, Wu GQ, Ge N, Li HP, Bao CY (2010) Volt-ampere and thermal features of a direct-current dual-jet plasma generator with a cold gas injection. IEEE Trans Plasma Sci 38(10):2906–2913
31. Huang Y, Yan Y (2000) Transient two-dimensional temperature measurement of open flames by dual-spectral image analysis. Trans Inst Meas Control 22(5):371–384
32. See http://physics.nist.gov/cgi-bin/ASD/lines1.pl for information about the upper energy level, statistical weight and Einstein transition probability at different wavelengths for Ar I lines
33. Coudert JF, Fauchais P (1997) Arc instabilities in a DC plasma torch. High Temp Mater Processes (New York) 1(2):149–166
34. Li TM, Choi S, Watanabe T (2012) Discharge characteristics of DC arc water plasma for environmental applications. Plasma Sci Technol 14(12):1097–1101
35. Lebouvier A, Delalondre C, Fresnet F, Cauneau F, Fulcheri L (2012) 3D MHD modelling of low current-high voltage DC plasma torch under restrike mode. J Phys D: Appl Phys 45(2):025204
36. Ghorui S, Vysohlid M, Heberlein J, Pfender E (2007) Probing instabilities in arc plasma devices using binary gas mixtures. Physical Rev E 76(1):016404
37. Dorier JL, Hollenstein C, Salito A, Loch M, Barbezat G (2001) Characterisation and origin of arc fluctuations in a F4 DC plasma torch used for thermal spraying. High Temp Mater Processes (New York) 5(4):477–489